Binding Patterns in Single-Ligand Complexes of NH_3, H_2O, OH^-, and F^- with First Series Transition Metals

Eric Magnusson* and Nigel W. Moriarty†

School of Chemistry, University College (ADFA), University of New South Wales, Canberra, ACT 2600, Australia

Received March 14, 1996[⊗]

Single-ligand complexes of first series transition metals with ammonia, water, hydroxide, and fluoride, many known in the gas phase, have been studied in calculations covering the 20 mono- and divalent cations and some very unusual binding patterns have been found. Binding energies and binding geometries were calculated at MP2 level, using a basis with a (6d/4d) contraction in the metal d space and 6-311+G** sets for the ligands. The results were used to distinguish the effect of steadily increasing nuclear charge across the series from the varying effects of d shell occupation. Even with only one ligand, the M^{2+} adducts displayed the familiar ligand field effects, d shell repulsion in the expected $d_\delta < d_\pi < d_\sigma$ order being superimposed on a regular progression to stronger binding and shorter bonds; that progression was disturbed only at the d^5 and d^{10} positions, when the d_σ orbital was occupied. Monovalent metal adducts behaved in strikingly different fashion, with irregular changes across early and late series metals in both bond length and bond strength. The irregularities are only partly attributable to the presence of both $d^{n-1}s$ and d^n ground states in the series. The other part of the explanation is the binding of anionic ligands inside the radial maximum of the 4s orbital. At these distances the normal binding preference shown by H_2O and NH_3 for d^n over sd^{n-1} cations is reversed. In contrast to steeply rising binding energies across the divalent metal ion adducts, the trend lines for the monovalent series are flat, the increments in nuclear charge being insufficent to offset the extra repulsion of electrons added to the d shell.

Gas-phase experiments on small metal−ligand adducts have opened up a new field of chemistry, offering the chance to carry out experimentally controlled calculations on transition metal complexes in a way which is impossible for larger compounds.[1] Although there are important differences between single-ligand adducts and the familiar four- and six-coordinate complexes, computational results for the small compounds obtained systematically at the same basis set level and degree of configuration interaction should help answer questions about metal−ligand bonding not easily tackled for the larger ones and on which experimental results are seriously incomplete. A major question is the effect on geometry and binding strength of different d orbital occupations. For small adducts this includes the effect of interchange between d^n and $d^{n-1}s$ configurations and states of mixed parentage.

The important work on adducts of first transition metal (TM) monocations carried out by Bauschlicher and co-workers[1−5] has been extended here to include doubly charged cations and other ligands, all treated at the same computational level. Part of the value of the earlier work is the persuasive rationalization by Rosi and Bauschlicher (RB) of the way in which ion−dipole binding is maximized and electronic repulsion minimized in ground and excited states of TM adducts of this kind.[3,4] The binding patterns are entirely consistent with electrostatic binding. For water adducts they order the strength of repulsion between water electrons and d electrons as follows but different orders must be expected for other ligands. The symmetry labels apply to the planar C_{2v} geometry; C_{2v} is optimum for all the TM M^{n+}-(H_2O) compounds.

$$M^+(H_2O):3d_{\delta'}\,(a_1) \sim 3d_\delta\,(a_2) < 3d_\pi\,(b_1) < 3d_{\pi'}\,(b_2) < 3d_\sigma\,(a_1)$$

We have already investigated the benefits of different kinds of basis sets and different levels of computation for TM compounds with a small number of ligands[5] and follow RB in using a 3111-contracted d function basis (six primitive d functions) because of its performance in distinguishing between different d^ns^m configurations. The wave functions were obtained at MP2 optimized geometries. Calculations of transition metal compounds are prone to serious error even at these levels, but we believe that we can estimate the effect of the errors and allow for them in conclusions drawn about trends in behavior across the TM series.

Computational Methods

The calculations, performed with the Gaussian 92 package[6] and with the MOTTEC codes,[7] are described in other papers.[1,8] Restricted and unrestricted Hartree−Fock and Moller−Plesset procedures (RHF, UHF, RMP2, UMP2) were used for closed and open shell systems respectively; in the MP2 level calculations the core electrons were not correlated.

The basis set used for the metal in these calculations ("Bausch") was derived from the Wachters basis[9] by RB; due to a software limitation, only one f function was used instead of RB's contraction of three f functions. No zero-point energy, spin−orbit coupling energy, or relativistic energy corrections were applied to the results here, which are relied on chiefly for the information they give about binding trends.

† Present address: Department of Theoretical Chemistry, Lund University, 221 00-Lund, Sweden

⊗ Abstract published in *Advance ACS Abstracts,* August 1, 1996.

(1) Bauschlicher, C. W., Jr.; Langhoff, S. R. In *Gas-Phase Metal Reactions*; Fontijn, A., Ed.; Elsevier Science Publishers BV: Amsterdam, 1992; pp 277−299.
(2) Langhoff, S. R.; Bauschlicher, C. W., Jr. *Annu. Rev. Phys. Chem.* **1988**, *39*, 181−212.
(3) Rosi, M.; Jr, Bauschlicher, C. W., Jr. *J. Chem. Phys.* **1989**, *90*, 7264−7272.
(4) Rosi, M.; Bauschlicher, C. W., Jr. *J. Chem. Phys.* **1990**, *92*, 1876−1878.
(5) Magnusson, E.; Moriarty, N. W. *J. Comput. Chem.* **1993**, *14*, 961−969.
(6) Frisch, M. J.; Trucks, G. W.; Head-Gordon, M.; Gill, P. M. W.; Wong, M. W.; Foresman, J. B.; Johnson, B. G.; Schlegel, H. B.; Robb, M. A.; Replogle, E. S.; Gomperts, R.; Andres, J. L.; Raghavachari, K.; Binkley, J. S.; Gonzalez, C.; Martin, R. L.; Fox, D. J.; Defrees, D. J.; Baker, J.; Stewart, J. J. P.; Pople, J. A. *Gaussian 92*; Gaussian, Inc.: Pittsburgh, PA, 1992.
(7) Clementi, E.; Roos, B.; Salez, C.; Veillard, A.; Gianolio, L.; Pavani, R.; Chakravorty, S. J. MOTECC Club, Kingston, NY, 1991.
(8) Magnusson, E.; Moriarty, N. W. Unpublished results.
(9) Wachters, A. J. H. *J .Chem. Phys.* **1970**, *52*, 1033−1036.

S0020-1669(96)00288-1 CCC: $12.00

Table 1. Binding Energies (kJ mol^{-1}) and (in Brackets) Metal−Ligand Distances (pm) of Single-Ligand Complexes of Monovalent Transition Metal Cations to NH_3, H_2O, OH^-, and F^- (for MP2 Optimized Calculations Using "Bausch" and 6-311+G** Basis Sets See Ref 8)

M^+		r_{rms}	$M^+(NH_3)$ BE [r_{MN}]	$M^+(H_2O)$ BE [r_{MO}]	$M^+(OH^-)$ BE [r_{MO}]	M^+F^- BE [r_{MF}]
K^+	s^0d^0	234.3	76.4 [289.3]	71.9 [271.9]	548.8[235.1]	453.0 [235.1]
Ca^+	sd^0	296.0	108.8 [266.4]	72.9 [303.9]	724.9 [219.3]	630.6 [252.4]
Sc^+	sd	292.2	169.2 [235.6]	140.4 [225.9]	879.8 [193.2]	834.1 [196.3]
Ti^+	sd^2	286.5	168.3 [228.4]	141.4 [216.8]	872.6 [188.9]	829.5 [188.4]
V^+	sd^3	280.7	178.0 [217.3]	135.3 [211.0]	855.6 [184.8]	815.4 [185.9]
Cr^{+*}	d^5	242.2	168.0 [219.1]	124.7 [216.7]	797.3 [185.9][a]	729.3 [180.1]
Mn^+	sd^5	270.4	171.7 [227.8]	134.2 [219.8]	858.7 [186.7]	815.0 [187.7]
Fe^+	sd^6	266.3	179.6 [220.7]	135.7 [214.2]	885.4 [183.5]	843.6 [183.1]
Co^+	d^8	235.2	213.3 [204.4]	152.6 [203.8]	817.7 [184.1]	759.5 [183.6]
Ni^+	d^9	232.0	235.2 [199.2]	170.1 [198.0]	847.0 [178.2]	778.9 [176.6]
Cu^+	d^{10}	228.4	230.0 [196.1]	157.8 [197.1]	844.2 [179.3]	782.4 [178.9]
Zn^+	sd^{10}	251.6	196.3 [210.1]	137.2 [207.6]	889.6 [183.6]	836.5 [180.9]

[a] The Cr^+OH^- value is an estimate based on unconverged MP2 calculations. The sd^4 state yields a binding energy of 766.4 kJ mol^{-1} at a binding distance of 183.1 pm.

Table 2. Binding Energies (kJ mol^{-1}) and (in Brackets) Metal−Ligand Distances (pm) of Single-Ligand Complexes of Divalent Transition Metal Cations to NH_3, H_2O, OH^-, and F^- (MP2 Optimized Calculations Using "Bausch" and 6-311+G** Basis Sets)

M^{2+}		r_{rms}	$M^{2+}(NH_3)$ BE [r_{MN}]	$M^{2+}(H_2O)$ BE [r_{MO}]	$M^{2+}(OH^-)$ BE [r_{MO}]	$M^{2+}F^-$ BE [r_{MF}]
Ca^{2+}	d^0	207.6	228.3 [254.2]	194.7 [247.9]	1247.0 [210.5]	1156.1 [220.6]
Sc^{2+}	d^1	213.6	317.6 [230.2]	271.4 [217.8]	1511.0 [185.5]	1426.5 [187.1]
Ti^{2+}	d^2	215.5	340.3 [222.5]	285.2 [209.6]	1519.7 [182.1]	1444.7 [181.3]
V^{2+}	d^3	214.9	372.8 [215.1]	303.5 [205.8]	1573.8 [175.6]	1479.8 [175.9]
Cr^{2+}	d^4	213.0	421.4 [207.7]	340.1 [198.9]	1625.3 [176.4]	1545.9 [174.0]
Mn^{2+}	d^5	211.4	405.1 [212.8]	325.4 [202.8]	1590.5 [177.3]	1498.4 [178.4]
Fe^{2+}	d^6	210.6	437.7 [206.0]	347.1 [197.4]	1655.7 [173.6]	1559.2 [173.9]
Co^{2+}	d^7	209.6	462.2 [201.2]	358.8 [193.2]	1672.6 [174.4]	1560.3 [174.3]
Ni^{2+}	d^8	208.4	498.7 [196.9]	380.7 [190.6]	1711.8 [172.3]	1592.8 [173.5]
Cu^{2+}	d^9	205.6	548.2 [191.5]	416.9 [186.0]	1781.7 [171.5]	1662.2 [169.6]
Zn^{2+}	d^{10}	203.4	520.1 [196.6]	389.8 [189.5]	1742.4 [177.9]	1618.9 [173.9]

RB's estimates of the size of these contributions to metal−ligand binding energies suggest that the main effect of ignoring them will be found for $d^{n-1}s$ rather than d^n configurations, s orbital energies tending to be exaggerated in the former.[3] Comparison with published values is possible for the monovalent (RB) and divalent[10] aquo adducts and the monovalent ammono adducts,[11] and the results are closely similar.

The difference between unrestricted Hartree−Fock and correlated wave functions is usually fairly small for metal complexes which are mainly electrostatically bound. One difference is the optimized metal−ligand bond distance; at MP2 level it is usually shorter than at HF level for these adducts which is the reverse of the case for bond distances calculated for ordinary covalently bound molecules. A second difference is metal orbital occupations. At the Hartree−Fock level s, p, and d orbitals mix and a state of a d^n configuration will have, e.g., an orbital with s and dσ contributions. MP2 and QCISD calculations on the same system allow contributions from sd^{n-1} states alongside the dominant d^n state contribution allowing some leakage of the d population to the s sub-shell, thereby reducing repulsion by d electrons. Configuration interaction calculations departed most from the HF results for the metals with nearly-filled d shells, e.g., Co−Cu. The differences can be readily explained as the result of the incorporation of Bauschlicher's mechanisms, for example, mixing configurations which increase the 4s orbital density at the expense of the highly repulsive $3d_\sigma$ density.

In certain cases MP2 and QCISD(T) calculations alter the order of the HF states of the adducts, just as they do for the corresponding free ions. For example, there are parallel changes in the Co^+ and Co^+-(H_2O) states; at UHF level the $^5B_2$ (sd^7) is lowest but $^3A_1$ (d^8) is lowest in the MP2 and QCISD(T) calculations.

Results

The full computational results for the adduct ground states, covering 88 metal−ligand combinations, are reported elsewhere[5,8] but the data needed for discussion here (binding energies and metal−ligand distances from MP2 level geometry-optimized calculations) are recorded in Tables 1 and 2 and displayed in the figures. There is one uncertainty in the data—the binding energy entry for the d^5 state of CrOH in Table 1 had to be estimated from unconverged MP2 calculations.

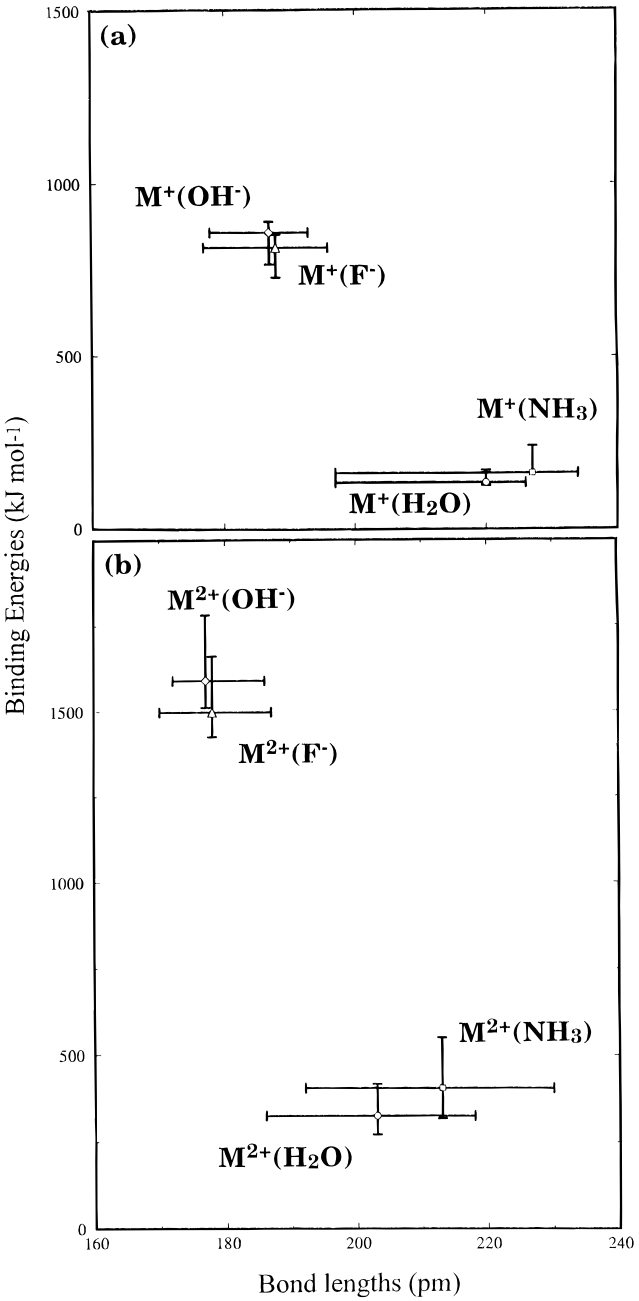

Figure 1. Minimum/maximum binding energies (kJ mol^{-1}) and binding distances (pm) of single-ligand adducts for the full transition metal ion series ($M = Sc^{n+}-Zn^{n+}$) and for Mn^+ and Mn^{2+} for (a) monovalent and (b) divalent transition metal ion adducts of the ligands NH_3, H_2O, F^-, and OH^-. Minima/maxima are indicated by vertical and horizontal bars (MP2 optimized calculations; "Bausch", 6-311+G** basis sets).

Figure 1 presents the range of variation of binding energies and distances for the mono- and divalent series, both drawn on the same scale. Figures 2−5 show the positions of the energy minima in plots of binding energy against metal−ligand bond length. These data are superimposed on the potential energy curves drawn for binding to the half-filled and filled d shell members of the two metal ion series; the divalent ion representatives are Mn^{2+} and Zn^{2+}. In the monovalent case two pairs are needed, for the d^n and sd^{n-1} categories: Mn^+ and Zn^+ (sd^5 and sd^{10}); Cr^+ and Cu^+ (d^5 and d^{10}). Note that four of the five

(10) Akesson, R.; Pettersson, L. G. M. *Chem. Phys.* **1994**, *184*, 85−95.
(11) Langhoff, S. R.; C W Bauschlicher, J.; Partridge, H.; Sodupe, M. *J. Phys. Chem.* **1991**, *95*, 10677−10681.

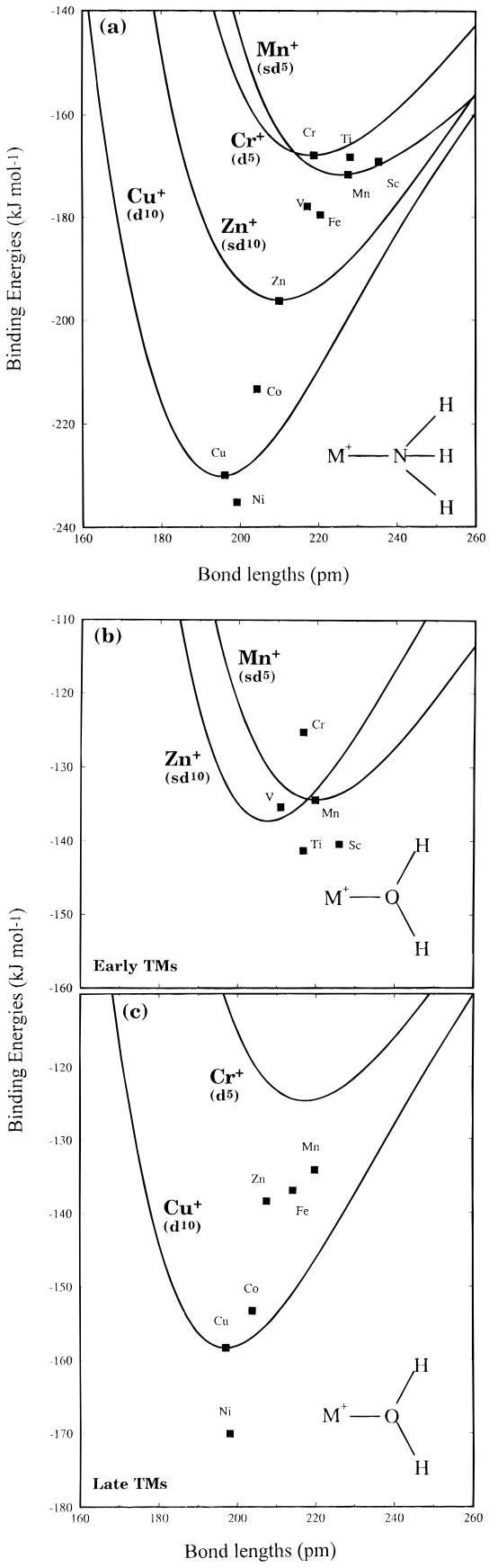

Figure 2. Binding energies (kJ mol^{-1}) and binding distances (pm) for (a) $M^+(NH_3)$ and $M^+(H_2O)$ adducts of (b) early and (c) late transition metal ions (MP2 optimized calculations; "Bausch", 6-311+G** basis sets; PE curves for the d^5, sd^5, d^{10} and sd^{10} members of the series drawn from single point MP2 results).

early TM monocations belong to the sd^{n-1} configuiration while the late TM monocations are mostly d^n.

Figures 6−8 display binding energies and distances plotted separately against position in the TM series. Figures 6 and 7 display the binding energies of the four sets of cation−ligand combinations, for mono- and dipositive metal ions respectively. The rms radii of the cations and the binding distance variations displayed by the two categories of M^+ ion adducts are given in Figure 8.

To understand their behavior, the adduct ground states of the TM series metals must be subdivided into three categories: d^n configurations for the divalent metal ion adducts, and, in the monovalent adducts, adducts with $d^{n-1}s$ and d^n ground states. The ground state adducts of all of the ligands belong to the same configurations and these, in turn, are derived from the high spin ground state of the free ion.

	Sc	Ti	V	Cr	Mn	Fe	Co	Ni	Cu	Zn
M^+	sd	sd^2	sd^3	d^5	sd^5	sd^6	d^8	d^9	d^{10}	sd^{10}
M^+ state	^3D	^4F	^5D	^6S	^7S	^6D	^3F	^2D	^1S	^2S
M^{2+}	d	d^2	d^3	d^4	d^5	d^6	d^7	d^8	d^9	d^{10}
M^{2+} state	^2D	^3F	^4F	^5D	^6S	^5D	^4F	^3F	^2D	^1S

The main features of the cation−ligand binding displayed by the adduct ground states can be summarized as follows.

(a) The single ligand bond energies reported here for TM ions are up to 50% greater than mean values for the corresponding hexacoordinated complexes. On the other hand, K^+ and Ca^{2+} bind so weakly to single ligands[12] that it is pointless to use them in comparisons with TM cation binding. Binding energies increase sharply in the step between the K^+ and Sc^+ adducts and then climb only slightly or not at all over the rest of the TM series. For the divalent metal ions, binding energies also leap in the d^0-d^1 step ($Ca^{2+}-Sc^{2+}$), but the subsequent rise over the remaining TM cations is quite small. Averaged across the TM series these MP2 level calculated binding energies (standard deviations) are as follows:

BE (kJ mol^{-1})	NH_3	H_2O	OH^-	F^-
M^+ series	191.0 (24.9)	142.9 (12.7)	851.7 (35.2)	802.4 (36.1)
M^{2+} series	432.4 (72.4)	341.9 (44.4)	1638.4 (86.7)	1538.9 (72.2)

(b) The differences in the binding abilities of the four ligands are much greater than the variations in binding between individual TM ions with any one ligand. The binding orders for the ligands are strikingly similar for all TM cations, in both the mono- and divalent cases. RB concluded that the binding of water and ammonia to monovalent TM cations is predominantly electrostatic. The similarities found here strongly suggest that the other compounds examined here are also mainly electrostatic. Covalent contributions to binding, if they are present, are mimicking the behavior so conveniently explained by a polar molecule simultaneously attracted to a cation and repelled by its d electrons. The detail of metal−ligand binding is reserved for discussion elsewhere[8] but, for the sake of simplicity, the adducts will be treated here as cation−dipole and cation−anion combinations.

Ammonia binds about 20% more strongly than water for both sets of cations (M^+ and M^{2+}). In the contest between fluoride and hydroxide ions the M^-OH binding is the stronger—by about 5% in both M^+ and M^{2+} series. Metal binding to anions is much stronger than to neutrals: $M^{+-}OH$ bond strengths are 4.4 (0.6) times as great as $M^{+-}NH_3$ values and $M^{2+-}OH$ bond strengths are 3.9 (0.5) times those of the $M^{2+}-NH_3$ compounds.

(c) Calculated optimum metal−ligand distances trend downward from Sc to Zn for all ligands, passing through the familiar minima in each half of the series. The calculated M−L distances are much shorter than experimental values in hexacoordinated metal complexes; the experimental M−O bond

(12) Magnusson, E. *J. Phys. Chem.* **1994**, *98*, 12558−12569.

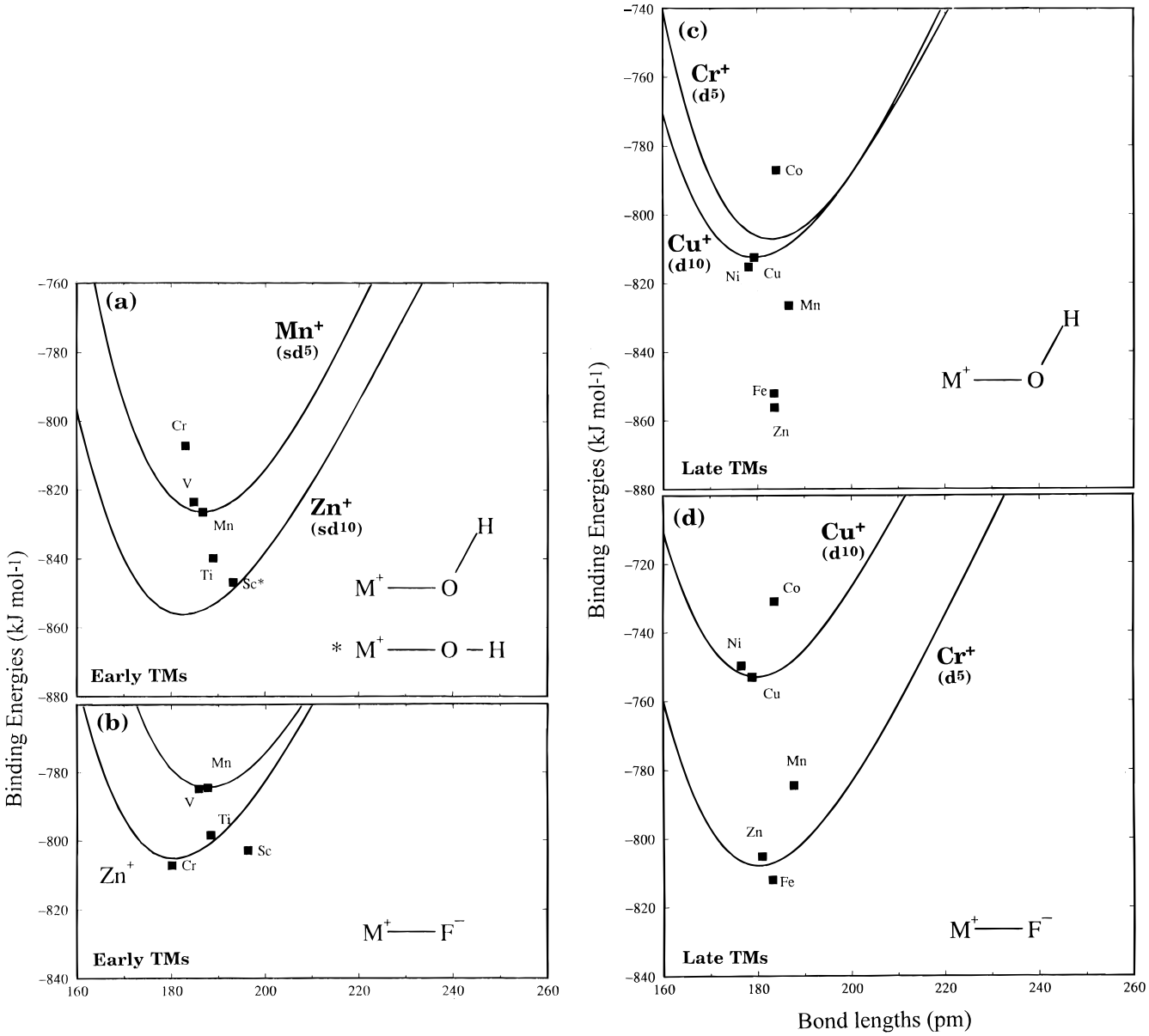

Figure 3. Binding energies (kJ mol^{-1}) and binding distances (pm) for $M^+(OH^-)$ and M^+F^- adducts of early transition metal ions (a and c) and late transition metal ions (b and d) (MP2 optimized calculations; "Bausch", 6-311+G** basis sets; PE curves for the d^5, sd^5, d^{10}, and sd^{10} members of the series drawn from single point MP2 results).

distances for the hexaqua transition metal ions cited in Akesson et al.[13] and Cotton et al.[14,15] are 3−11% larger (up to 20 pm) than the values calculated here. If for no other reason, mutual repulsion between polar or anionic ligands attached to the same cation will lead to increases in bond distances and a fall in binding energies as extra ligands are added. The experimental data are scarce for ligands other than water but the picture is the same. For example, the metal−ligand distances listed for Cu(II) in the compilation of Orpen et al.[16] are larger by 4% (NH_3), 12% (OH^-), and 14% (F^-) than the distances reported here.

Averaged across the TM series these MP2 level calculated binding distances (standard deviations) for the single ligand adducts are as follows:

r_{ML} (pm)	NH_3	H_2O	OH^-	F^-
M^+ series	215.9 (12.5)	211.1 (8.9)	184.5 (4.1)	184.2 (5.4)
M^{2+} series	208.1 (11.6)	199.2 (9.4)	176.7 (4.1)	176.2 (4.7)

As for binding energies, the binding geometries of the TM ions are quite different from those of the adducts formed by K^+, Ca^+, and Ca^{2+}.[12] Unexpectedly, in the case of the neutral ligands the more weakly bound ligand is calculated to bind closer to the metal ion and by an amount greater than the difference between the radii (0.75 Å for N and 0.73 Å for O). Although the more weakly binding ligand, F^-, binds closer than OH^-, the difference is readily accounted for by the difference in the O and F radii.

Discussion

The main interest in these computational results centers on the variable relationship between binding energies and binding geometries and, in particular, the unexpected contrast between the energy/distance patterns of the M^+ and M^{2+} series. The binding patterns are discussed in points a−e below, and a rationalization of "regular" and "irregular" patterns is attempted in point f.

(a) Baseline Energy and Distance Trends. Before introducing other variables which may affect the results in Figures

(13) Akesson, R.; Pettersson, L. G. M.; Sandstrom, M.; ; Siegbahn, P. E. M.; Wahlgren, U. *J. Phys. Chem.* **1992**, *96*, 10773−10779.

(14) Cotton, F. A.; Daniels, L. M.; Murillo, C. A.; Quesada, J. F. *Inorg. Chem.* **1993**, *32*, 4861−4867.

(15) Cotton, F. A.; Daniels, L. M.; Murillo, C. A. *Inorg. Chem.* **1993**, *32*, 4868−4870.

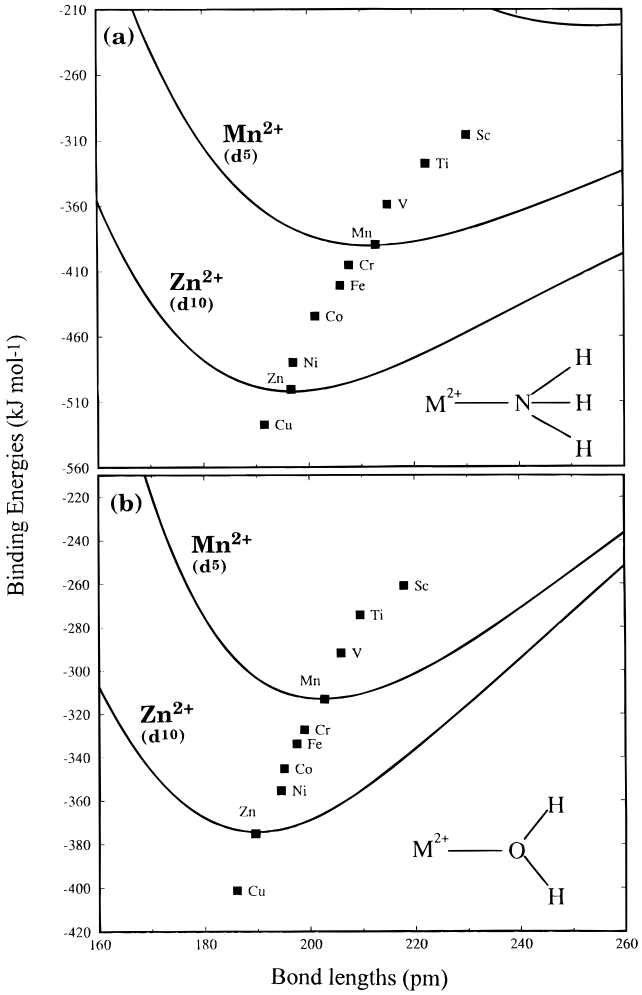

Figure 4. Binding energies (kJ mol^{-1}) and binding distances (pm) for (a) $M^{2+}(NH_3)$ and (b) $M^{2+}(H_2O)$ adducts of transition metal ions (MP2 optimized calculations; "Bausch", 6-311+G** basis sets; PE curves for the d^5 and d^{10} members of the series drawn from single point MP2 results).

2−5, it is useful to consider the adducts with all d orbitals equally occupied. These cases provide the baselines on which the different effects of the occupation of d_σ, d_π, and d_δ orbitals are superimposed; they appear as broken lines in Figures 6 and 7.

In the monovalent series, where six out of ten adducts retain sd^n ground states, the "baseline" configurations are sd^5 and sd^{10} (Mn^+ and Zn^+); Ca^+, the sd^0 case, is not included because it binds too weakly. For the divalent series the baseline is provided by the d^5 and d^{10} cases (Mn^{2+} and Zn^{2+}), and again, Ca^{2+} is not included.

The data below summarize the changes in binding energy and optimum M−L bond distance for the eight series of adducts. Data for hexacoordinated metal complexes for comparison with these are hard to find. For water complexes of divalent TM series metals the hydration enthalpies in solution[17] rise by 11% between Mn^{2+} and Zn^{2+} compared with a 20% increase for the single-ligand binding energies reported here.

	Mn^+/Zn^+ (sd^5/sd^{10})		Mn^{2+}/Zn^{2+} (d^5/d^{10})	
	ΔE (kJ mol^{-1})	Δr_{ML} (pm)	ΔE (kJ mol^{-1})	Δr_{ML} (pm)
NH_3	+24.6	−17.7	+115.0	−16.2
H_2O	+ 3.0	−12.2	+ 64.4	−13.3
OH^-	+30.9	−3.1	+151.9	−0.6
F^-	+21.5	−6.8	+120.5	−4.5

Δr_{ML} values for hexacoordinated metal ions are hard to obtain, but the use of Shannon and Prewitt radi for Mn^{2+} (97 pm) and Zn^{2+} (88 pm)[18,19] would suggest a value of ≈9 pm for Δr_{ML}.

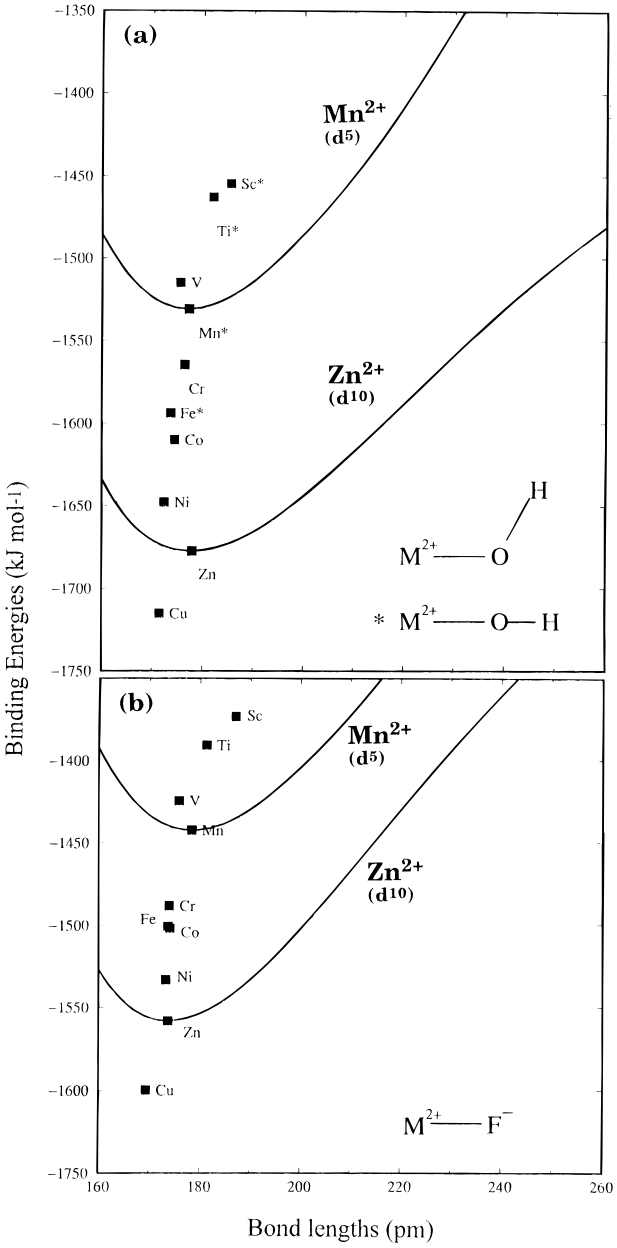

Figure 5. Binding energies (kJ mol^{-1}) and binding distances (pm) for (a) $M^{2+}(OH^-)$ and (b) $M^{2+}(F^-)$ adducts of transition metal ions (MP2 optimized calculations; "Bausch", 6-311+G** basis sets; PE curves for the d^5 and d^{10} members of the series drawn from single point MP2 results).

The Cr^+, Co^+, Ni^+, and Cu^+ members of the monovalent series have d^n configurations. This subset includes the d^5 and d^{10} members of the series and their behavior can be related to a baseline drawn between Cr^+ and Cu^+. The data for the M^+OH^- series are based on the estimated binding energy of the d^5 Cr^+OH^- adduct given in Table 1.

	$Cr^+/Cu^+(d^5/d^{10})$	
	ΔE (kJ mol^{-1})	Δr_{ML} (pm)
NH_3	+62.0	−23.0
H_2O	+33.1	−19.6
OH^-	+46.9	−6.6
F^-	+53.1	−1.2

Although many variations in pattern are visible in the binding energy/bond length plots, these results show the baseline

(16) Orpen, A. G.; Brammer, L.; Allen, F. H.; Kennard, O.; Watson, D. G.; Taylor, R. *J. Chem. Soc., Dalton Trans.* **1989**, S1−S83.
(17) Smith, D. W. *J. Chem. Educ.* **1977**, *54*, 540.
(18) Shannon, R. D. *Acta Crystallogr.* **1976**, *A 32*, 751−767.
(19) Shannon, R. D.; Prewitt, C. T. *Acta Crystallogr.* **1969**, *B25*, 925−945.

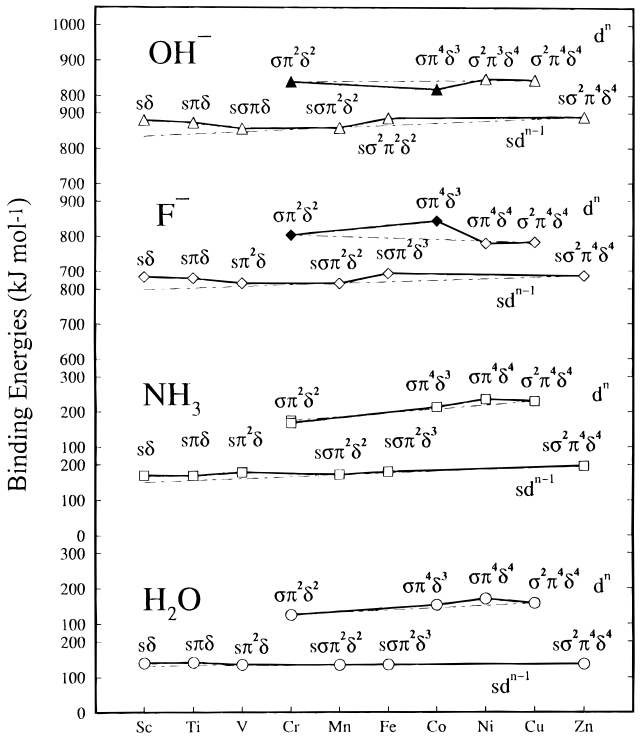

Figure 6. Binding energies (kJ mol^{-1}) for monovalent cation adducts M^+L (L = NH_3, H_2O, OH^-, F^-) plotted against position in the first transition metal series and d orbital occupations ("s" = 4s; "σ, π, δ" = d_σ, d_π, d_δ). Adducts with d^n ground states are plotted on the same scale but offset above the sd^{n-1} state adducts . Dotted lines indicate trends drawn between the sd^5 and sd^{10} members (for the sd^{n-1} sequences) and between the d^5 and d^{10} members (for the d^n sequences).

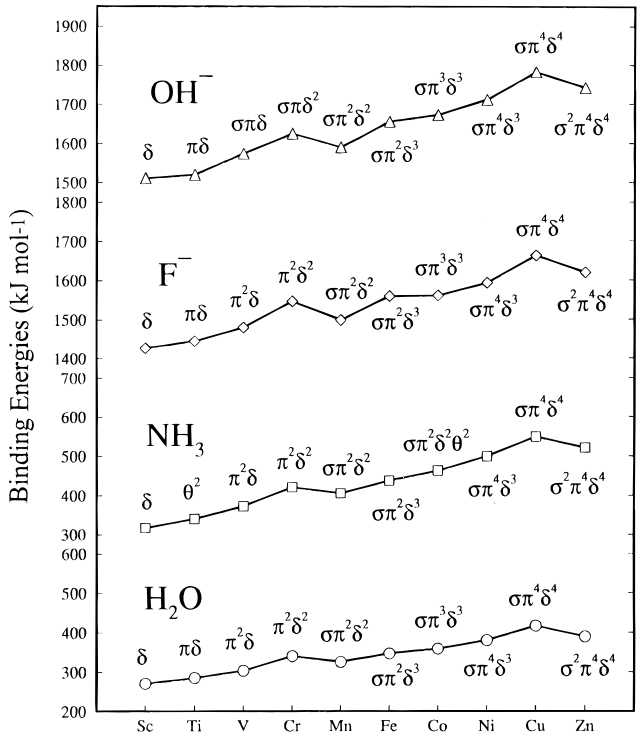

Figure 7. Binding energies (kJ mol^{-1}) for divalent cation adducts $M^{2+}L$ (L = NH_3, H_2O, OH^-, F^-) plotted against position in the first transition metal series. The d orbital occupations, all d^n, are shown ("σ","π","δ" for d_σ, d_π, d_δ).

behavior to be fairly uniform: the trend across the TM series toward stronger, shorter bonds is adhered to in all 12 series.

Several features stand out of the baseline comparisons. First, the degree of bond shortening associated with the anionic ligands—it is only about one-fifth of the shortening seen in the

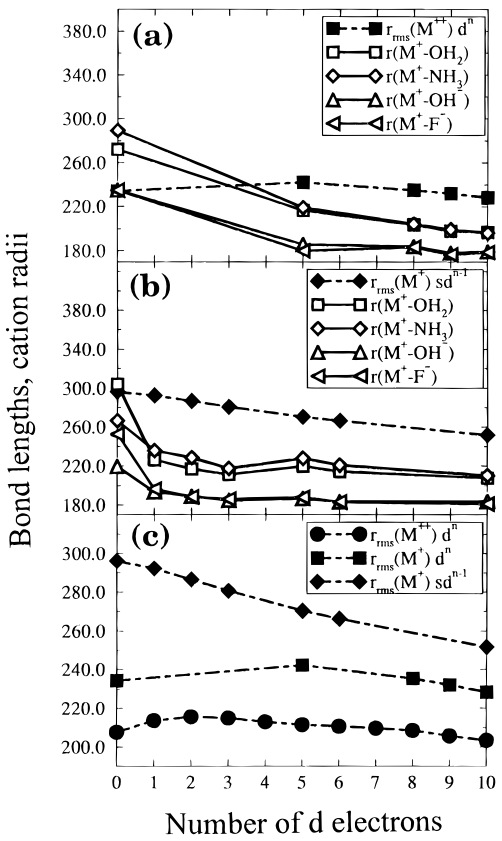

Figure 8. Metal ion radii and bond lengths of metal ion adducts with H_2O, NH_3, OH^-, and F^- plotted against d-electron number: bond lengths [r(M−L)] of compounds with d^n ground states (a) and compounds with sd^{n-1} ground states (b) and cation radii [$r_{rms}(M^{n+})$] (c).

monovalent water and ammonia adducts. In the d^ns case, the bond in zinc(I) fluoride is actually slightly longer than the Cr(I)−F bond. Secondly, the M^+ bond energy baselines are only about one fifth as steep as the M^{2+} baselines (mean values). For the M^+ series the the full effect of nuclear charge (d^1 to d^{10} and sd^1 to sd^{10}) on bond energy is no larger than the deviations from it (see Figures 5 and 6); in the M^{2+} series it greatly exceeds the deviations.

(b) Binding Energy vs d-Orbital Occupation Trends. In all cases the binding energy progressions in Figures 6 and 7 conform to the familiar "double-humped" pattern—ligand field energy contributions superimposed on a trend based on the two cases (d^5, d^{10}) in which the d-shell configuration precludes ligand field stabilisation.

The plots of binding energy against d orbital occupation in Figures 6 and 7 suggest that the monovalent adduct behavior is analogous to that of the divalent ion adducts and give no hint that binding distance behaves as a second independent variable. Considering how different is the bond length response to d electron occupation in anionic and neutral ligand adducts, it is remarkable that the binding energy dependence hardly changes. The only point at which the parallelism breaks down is at the d^9 representative, where the Ni^+F^- binding energy fails to rise above the d^5−d^{10} baseline.

(c) Ligand Effects on Binding Energy/Distance Patterns. The trends in Figures 4 and 5 for adduct formation between divalent cations and ligands are strikingly different from, and simpler than, those in most of the monovalent ion datasets in Figures 2 and 3. They are summarized here, divalent ion adduct patterns being described first.

$M^{2+}(NH_3)$ and $M^{2+}(H_2O)$. For these two ligands the behavior of the adducts is "regular", this epithet being applied

to the progression toward the bottom left of the plot—to stronger, shorter bonds. It includes the fact that in the early (d^1-d^5) and late (d^6-d^{10}) TM sequences the shortest and strongest bonds are formed at Cr^{2+} and Cu^{2+}, d^4 and d^9, respectively. For the spin-coupled d^5 configuration of Mn^{2+} and the filled d shell of Zn^{2+} strong repulsion between the ligand lone pair and the d_σ electron(s) is unavoidable.

$M^{2+}(OH^-)$ and $M^{2+}(F^-)$. The progressions for the divalent hydroxide and fluoride adducts are strange because they are almost vertical: it is as if the ligand at this close approach to the metal is up against a wall, displaying a broad range of binding energies but little corresponding bond length variation. Apart from this feature, and the unusual position of the $Ti^{2+}OH^-$ adduct (probably due to its linear geometry when most other members of the series are bent) the behavior is "regular", Mn^{2+} (d^5) and Zn^{2+} (d^{10}) each again occupying the penultimate position in the respective half of the series.

$M^+(NH_3)$ and $M^+(H_2O)$. The plots obtained for these two ligands with the early TMs are "circular" and very similar. The bonds for the sd^2-sd^5 cases are all shorter than the sd^1 Sc^+-L bond, as expected, but the bond energies never go lower than those of Ti^+ and Sc^+. The patterns which the late TM cations exhibit in the water and ammonia adducts are fairly distinctive and could be characterized as a "regular" sequence (progression to stronger, shorter bonds), but there is a strong reversal of behavior when the d shell is almost full, the bonds to Cu^+ and Zn^+ both being much weaker than those to the preceding cations. However, the adducts lie in two groups whose positions are correlated with their category. The d^8,d^9 and d^{10} cases (Co^+, Ni^+, Cu^+) lie in a cluster to the lower left of the adducts with sd^5, sd^6, and sd^{10} configurations (Mn^+, Fe^+, Zn^+).

$M^+(OH^-)$. For this set of adducts the points lie in sequence, but the trend from Sc^+ to Cr^+ is toward weaker bonds even though they become progressively shorter! Consistent with this sequence the Mn^+ adduct appears at an intermediate and not a terminal position, and the Cr^+ adduct, with its d^5 configuration, displays the weakest binding. An explanation is needed, however, for the shortness of the Cr−O bond. In behavior which is the opposite of the H_2O and NH_3 adducts, the late TM ions here show the Co^+, Ni^+, and Cu^+ (d^8, d^9 and d^{10}) cluster above Mn^+, Fe^+, and Zn^+ (sd^5, sd^6 and sd^{10} states) points and, with only minimal binding distance variations, "vertical". The d^9 adduct is lower in energy than the d^{10} adduct, as usual, but only marginally so. These unusual movements in binding can be visualized in Figure 5; binding energies of the late TM series M^+OH^- and M^+F^- adducts drop below the d^5-d^{10} trend lines, a feature not seen for any other adduct series.

$M^+(F^-)$. The early TM metal adducts display the "circular" pattern found for the water and ammonia compounds, and the late series adducts conform to the same almost "vertical" pattern shown by the M^+OH^- adducts.

(e) Isoelectronic Sequences. The data for the M^+ d^n adducts provide $d^5-d^8-d^9-d^{10}$ sequences for monovalent metal ions with each of the four ligands. When these adducts are compared with the $d^5-d^8-d^9-d^{10}$ cases from the M^{2+} adduct series, the similarity is strong: the differences between metal oxidation states are only differences in magnitude, not pattern. The only deviations occur for the monovalent OH^- and F^- adducts and then only by a failure to exhibit the drop in strength of binding, and the parallel change in bond length, at the last step.

The remaining adduct energies and bond distances from the monovalent series results allow a similar examination of $d^{n-1}s$ sequences. Comparison between the mono- and divalent series is still possible but of adduct ground states which are not isoelectronic. The datasets are those of the $d^3-d^4-d^6-d^7$ and $d^2s-d^3s-d^5s-d^6s$ sequences which occur with Ti^+/V^{2+} (d^2s and d^3), V^+/Cr^{2+} (d^3s and d^4), Mn^+/Fe^{2+} (d^5s and d^6) and Fe^+/Co^{2+} (d^6s and d^7). Even here, however, the similarity in binding between the two anions and between the two neutrals remains the most prominent feature.

Comparing the trends in the four series of M^{2+} adducts with the corresponding M^+ compounds makes it clear that the effects of individual metal electron configurations on the bonding in the M^+ adducts are swamped in the M^{2+} series adducts by the effect of the effective nuclear charge, which increases steeply across the TM series.

(e) Electron Density Distributions of the Adducts. Not all of the differences between the binding patterns for four ligands in the monovalent and divalent series are discernible in the population data. As indicated by Mulliken populations, charge transfer is greater from anionic than from neutral ligands and to divalent than monovalent cations. The atomic charges (q_M) on the metal ions vary by a surprisingly small amount across the series, as shown by the means (standard deviations):

	L = NH_3	L = H_2O	L = OH^-	L = F^-
q_M in $[M^+L]$	0.78 (0.04)	0.85 (0.03)	0.47 (0.07)	0.51 (0.05)
q_M in $[M^{2+}L]$	1.45 (0.12)	1.66 (0.05)	1.18 (0.11)	1.25 (0.04)

The q_M values are slightly more constant across the monovalent TM series than across the M^{2+} compounds; the variance is mainly due to falling q_M values in the latter and oscillating q_M values in the former. Adding one nuclear charge is almost exactly offset by the adding of one d electron at each step across the series of monovalent ions (efficient shielding) but not in the divalent ions (inefficient shielding) and accords with the respective "horizontal" and "rising" trends in the binding (see Figures 5 and 6).

For both the monovalent and divalent series, the Mulliken charge s and p orbital densities q_s and q_p are larger for the late TM ions than for the early series members. Hybridization allows repulsion between ligand and metal electrons to be minimized which becomes more important when the d shell occupation is higher. The reverse effect can be seen in the data for the d orbitals where the nonintegral part of q_d is partly due to d electron contributions to bonding orbitals. These drop sharply in the late TM ions. The relation holds for all four ligands, even though charge transfer is much greater for OH^- and F^- adducts than for H_2O and NH_3. The q_d values (MP2 calculations) for the early and late $M^{2+}(H_2O)$ and $M^{2+}OH^-$ adducts follow:

	d^1	d^2	d^3	d^4	d^5
$Sc^{2+}(H_2O)-Mn^{2+}(H_2O)$	1.10	2.10	3.11	4.12	5.05
$Sc^{2+}OH^--Mn^{2+}OH^-$	1.44	2.52	3.43	4.41	5.17
	d^6	d^7	d^8	d^9	d^{10}
$Fe^{2+}(H_2O)-Zn^{2+}(H_2O)$	6.07	7.06	8.05	9.12	10.01
$Fe^{2+}OH^--Zn^{2+}OH^-$	6.23	7.20	8.17	9.22	10.03

In the $Sc^{2+}OH^-$ adduct, the value of 1.44 comes from individual orbital populations of $d_\sigma^{0.14}d_\pi^{0.15}d_{\pi'}^{0.15}d_\delta^{0.0}d_{\delta'}^{1.0}$ probably due to minor bonding contributions from the d_σ and d_π orbitals while the other d electron occupies the least repulsive $d_{\delta'}$ orbital.

One feature of the binding energy/distance patterns of Figures 2−5 which is visible in the population data is the position of the end members of early and late TM ions. For the M^+ series the Mn^+ adducts adhere to the sd^5 configuration, and invariably the occupation of the d_σ orbital strongly inhibits the sd_σ mixing that occurs in Sc^+, Ti^+, V^+, and Cr^+ adducts and brings the d orbital population back closer to the integral value. Thus in the population data above for the water and hydroxy adducts the sharp change back to a q_d value close to integral is paralleled in all the other TM ion sequences, early and late.

(f) Rationalisation of the Irregular Binding Patterns in Monovalent Metal Ion Adducts. The divalent TM adducts

considered here inhabit a fairly strong binding domain where the increment in effective nuclear charge at each step across the TM series overwhelms interelectronic repulsion between ligands and the metal d shell and progressions are "regular". By contrast the M^+L series progressions include jumps to weaker but shorter bonds at some or all steps in the sequence Sc^+-Mn^+ and bond strength trends across the series are horizontal. The late TMs display major changes in binding energy with only very minor bond length variation—the "vertical" patterns. Although the range of energies over which the monovalent adducts bind is only half that of the divalent compounds, they still bind over the same wide range of distances (see Figure 1).

The binding energy advantage resulting from doubly charged cations in the $M^{2+}L$ series is accompanied by correspondingly large binding energy changes between neighbor elements in the transition metal sequence. This occurs because the $M^{2+}L$ series bonds are shorter, ligand electron pairs are much closer to the d shell, and repulsion energy differences between different d orbital occupations are much larger than they are in M^+L adducts. So, the fact that M^+L series binding energy differences are smaller than those of $M^{2+}L$ adducts is predictable but the size and the highly variable direction of Δr_{ML} in the early TM monovalent adducts is not. By contrast, the major variable in the adducts of the late TMs is bond energy. In both groups of these monovalent compounds a reason must be found for the disappearance of the usual strong correlation between bond distance and bond strength.

Clues to an explanation for the irregular behavior are easier to see when the strength and distance variations are given separately (Figures 6 and 8). Figure 8 introduces the rms free ion radii so that the differences between the sizes of the sd^{n-1} and d^n ions can be appreciated, and it also distinguishes between the two categories by presenting the metal−ligand distance plots separately. The existence of $d^{n-1}s$ as well as d^n configurations among both early and late TMs is part of the reason for the discontinuities in binding shown by the M^+L compounds, but it is not the whole reason.

The sizes of the three categories of TM ions, as revealed by the rms radii in Figure 8c, are distinctly different, and it is no surprise that the sd^{n-1} ions show smaller screening and larger size contraction across the TM series than the d^n set. The sd^{n-1} ions are also more severely deformed by attachment of ligands (see Figure 8). Nevertheless, the presence of the diffuse 4s electron still keeps the monovalent metal−ligand distance 10−20 pm longer for the sd^{n-1} than for the d^n ions and the latter 5−15 pm longer than r_{ML} for the M^{2+} adducts. The long metal−ligand bond in the sd^{n-1} case will be, therefore, much more sensitive than in the d^n case to changes in attractive and repulsive energy terms at each step across the TM series; irregular changes in binding distance are the result.

Bond length variation is strong for the early TM adducts. That the contractions we calculate for these compounds are a consequence of the various occupations of d_σ, d_π, and d_δ orbitals across the TM series and not a ligand property follows from the remarkable similarity in the patterns for the four ligands. Because OH^- and F^- are attached to the TM cations at distances less than 190 pm, even in the M^+L compounds, binding occurs in a much steeper region of the repulsive and attractive curves and changes in bond distance across the TM series are, on average, only one-fifth as great as the r_{ML} variations in the adducts of the neutrals. Nevertheless, a strong similarity in the pattern of binding for the TM series is preserved, as Figure 8 (b) makes obvious.

The positions of the Mn^+ and Cr^+ adducts deserve special mention. The plots of Figures 2, 3, and 8 show the Mn^+ adduct, always with the sd^5 configuration, to be generally in the middle of the other four early TM compounds. This occurs because the d_σ electron makes the bonds weaker than those formed by the preceding cations and longer than all except those to Sc^+. Cr^+ is the odd member in all sequences. Its position in the early TM series compounds is explained by its d^n configuration. The d^5 configuration makes the Cr^+ adduct the weakest of the early TM adducts, because of the forced occupation of the d_σ orbital. In spite of the weakness of the Cr−L bond, the absence of the 4s electron makes it among the shortest.

In a few cases in the monovalent series the kind of change produced by taking one step across the TM series is the same for all four ligands. Two such steps are $sd^5 \rightarrow sd^6$ ($Mn^+ \rightarrow Fe^+$) and $sd^2 \rightarrow sd^3$ ($Ti^+ \rightarrow V^+$). The former change (adding one d electron to the half-filled shell) makes all bonds shorter and stronger, and the $sd^2 \rightarrow sd^3$ change uniformly produces shorter, weaker bonds. Uniformity of this kind is as uncommon in the M^+ series adducts as it is common in the M^{2+} series and fails to appear even for steps where it would be most confidently predicted, e.g. at the $d^5 \rightarrow sd^5$ and $d^{10} \rightarrow sd^{10}$ steps. The conclusion must be that different ligands provide very different effects on energy for a one-step change. On the other hand, all the cases quoted had the same effect on bond distance!

It remains to explain the irregularities in the late TM monovalent ions—patterns dominated by changes in binding energy. That binding energy, rather than binding distance, is dominant for the OH^- and F^- adducts of the late TM ions is due to the fact that these ligands are so close to the metal ion. The variability of r_{ML} for the M^+H_2O and M^+NH_3 adducts is greater than that of the M^+F and M^+OH series, but size still varies less with position in the TM series than was the case for the early TMs and this is just a consequence of the size convergence expected at the end of the series as the ions become harder.

Superficially, the position of the anions 20 pm closer to the metal than neutral H_2O and NH_3 molecules makes no difference to the almost vertical pattern of binding with these TMs. However, in the case of the OH^- and F^- adducts, the sd^5, sd^6, and sd^{10} ions are bound 50−60 kJ mol^{-1} more strongly than the d^8, d^9, and d^{10} ions, quite the opposite of the situation for binding to NH_3 and H_2O. The explanation for this reversal is that OH^- and F^- ions are bound so far within the diffuse 4s orbital that its nuclear shielding effect is almost zero and the binding is stronger than that to the d^n ions. For water and ammonia at metal−ligand distances between 200 and 210 pm, the 4s electron cloud seriously interferes with binding and the sd^{n-1} ions form much weaker bonds than d^n ions.

The explanation for the d^n/sd^{n-1} reversal, that the 20−30 pm difference in bond distance between anionic and neutral ligands is enough to negate shielding of the TM nucleus by the 4s orbital can be tested. Taking H_2O and OH^- as examples, we compare the binding energies of d^n and sd^{n-1} TM cations for neutral and anionic ligands with binding by a point charge (Z^+) placed at the same distance from each ligand.

	ML	r_{ML}	BE (kJ mol^{-1})	Z^+L	BE (kJ mol^{-1})
d^{10}	Cu^+OH^-	179.3	844	Z^+OH^-	838
sd^{10}	Zn^+OH^-	183.6	820	Z^+OH^-	890
d^{10}	$Cu^+(H_2O)$	197.1	158	Z^+H_2O	163
sd^{10}	$Zn^+(H_2O)$	207.6	137	Z^+H_2O	155

Note that the anion, which is bound at close range, binds the d^{10} cation 101% as effectively as Z^+, the point positive charge. The sd^{10} cation reaches 108%, in spite of being 10 pm further away. In the case of water, the d^{10} cation is 97% as effective as Z^+ while the sd^{10} cation drops down to 89%. In other words, the 4s electron keeps water at a greater distance from the cation, simultaneously shielding the TM cation and reducing the binding

energy. With the hydroxide ion attached much further inside the diffuse 4s electron cloud the relative strength of binding of d^{10} and sd^{10} cations is completely reversed.

In the case of the hydroxo adducts, some of the irregularity is due to the angular dependence of binding of this ligand at short range. Repulsion can often be reduced slightly by changes in the angle of approach to the metal so bond angle changes are seen in both the monovalent and divalent metal ion sequences of hydroxide adducts. Since adjustment of the bond length is no longer the only way to the minimum of the energy surface it is understandable that bond length trends do not exactly follow those of the fluorides.

Summary

Electronic structure calculations of single ligand complexes of first transition series metal ions show striking differences in patterns of binding between neutral ligands (water, ammonia) and anions (hydroxide, fluoride) and between the monovalent and divalent metal ions. The properties of the M^+ and M^{2+} series adducts are rationalized on the basis of repulsion between ligand electrons and occupied s and d orbitals (increasing in the order $d_\delta < d_\pi < d_\sigma$) as found earlier by Bauschlicher et al. for two of the eight series studied here. When binding energies are considered alone, the adducts conform broadly to classical ligand field concepts; all display the familiar double-humped curve, and all have adducts with half-filled and filled d configurations forming weaker bonds than preceding members of the series.

When bond energy and bond distance are plotted together the "regular" progression across the TM series to stronger, shorter bonds is shown only by the $M^{2+}L$ adduct sequences. When early and late TMs are considered separately the 16 sequences studied here include many "irregular" patterns. Some are "vertical" (bond energies rise while bond lengths hardly change in five sequences of fluoride and hydroxide adducts), some are "reversed" (M^+OH^- adducts of the early TM ions show bond energies decreasing while bond lengths also decrease), and some are "circular" (early TM ion sequences of M^+NH_3 and M^+F^- adducts exhibiting bond lengths and bond energies which go down in parallel, and then up). These irregularities are partly attributable to the presence of sd^{n-1} as well as d^n configurations among M^+L series adducts, partly to novel behavior in the hydroxide and fluoride adducts. Bond distances are so small in the latter groups that the anions are embedded in the metal ions.

Metal−anion bond lengths cover the range 173−196 pm (mean 180 pm) compared with 186−230 pm (mean 208 pm) for bond lengths to the neutrals. The anions, attached well inside the rms radii of the diffuse 4s orbital, are bound 50−60 kJ mol^{-1} more strongly to M^+ cations with sd^{n-1} configurations than to the d^n cations even though there is little difference in binding distance. The binding preference for the more distant H_2O and NH_3 ligands is the opposite of this. Irregularities are absent from the divalent series adducts because the nuclear charge effect is sufficient at each step to shrink the bond and strengthen the binding, swamping opposing effects from progressive occupation of d orbitals. The d^4/d^5 and d^9/d^{10} steps are always exceptions to this rule. Because of the forced addition of a d_σ electron Mn^{2+} and Zn^{2+} can form only the second strongest adducts and have the second shortest bonds.

In spite of the discontinuities produced by d^n-sd^{n-1} configuration changes, by the very much closer approach of ligand to metal in OH^- and F^- than in H_2O and NH_3 adducts, and by a 6-fold difference in mean binding energy between the weakest and strongest binding ligand, the patterns of binding of the four ligands for TM cations are amazingly parallel. They are dominated by the d electrons, the effects of successive occupation of d_δ, d_π, and d_σ orbitals being far too strong to be disturbed by the individual characteristics of the ligands.

Acknowledgment. The research was supported by the Australian Research Council.

IC960288M